❒   50

A hybrid combination of improved mayfly optimization based modified perturb and observe for solar based water pumping system

Dattatray Surykant Sawant, Yerramreddy Srinivasa Rao, Rajendra Ramchandra Sawant
Department of Electronics and Telecommunication Engineering, Bharatiya Vidya Bhavan's Sardar Patel Institute of Technology,
Mumbai, India

ABSTRACT

In recent years, solar water pumping systems (WPS) have been fuel-free and environmentally beneficial because they have gained a lot of attention in the agricultural and industrial sectors. Traditional water pumps consume higher amount of energy which make it as frequently unreliable, low efficiency and needs high maintenance. For WPS applications, Brushless DC (BLDC) motors are far superior options than other induction motors because of their high efficiency, high dependability, and low maintenance needs. Thus, in this research, the major goal is to develop a more efficient, reliable, and maintenance-free solar WPS solution. This paper describes a sensorless control strategy that reduces the need for hall sensors and increases system's overall reliability. Solar system power is typically impacted by partial shadowing and cannot reach the maximum available power because the traditional perturbed and observe (P&O) algorithm fails. This paper integrates the modified P&O (MP&O) algorithm with an improved mayfly optimization (IMO) name called IMO-MP&O to address these issues by efficiently extracts the maximum power from solar. From the results, it clearly shows that IMO-MP&O achieved higher efficiency of 99.58% than the existing P&O MPPT which is analyzed the MATLAB sim-power-system toolboxes.

Corresponding Author:

Dattatray Surykant Sawant
Department of Electronics and Telecommunication Engineering
Bharatiya Vidya Bhavan's Sardar Patel Institute of Technology
Mumbai, India
Email: dssawant1@gmail.com

1. INTRODUCTION

Among all the renewable energy sources (RES) currently available, Solar energy is considered the most practical and effective harvesting because it could easily meet the world's current energy needs [1]. Solar-photovoltaic systems are becoming a competitive alternative for industrial, space-plane, agricultural, and residential applications [2], particularly for a country like India that receives a lot of sunlight but has a limited supply of fossil fuels. For the past few years, conventional cars have been using petroleum products, which has led to a global upsurge in environmental pollution and grave concerns [3]. To combat environmental pollution, vehicles with renewable energy sources like solar, fuel cells, and hybrid systems are being introduced [4]. Vehicles eventually became the greatest technological advancement in the automotive industry as a result. The motor in these vehicles requires an electric power source to operate [5]. This power source is made up of a battery that, once completely depleted, needs to be recharged [6]. This suggests that

battery-powered electric cars' driving range could be limited, requiring regular battery charging. To overcome the aforementioned problems, PV has been selected as an excellent battery substitute [7]. PV shows respectable accuracy and illustration during the steady-state procedure; however, its response time in transient conditions is insufficient [8]. Modernization and the expansion of human society depend on electric drives. Over 40% of power is used in electrical drive which is consumed by motors [9]. For this reason, motors are essential in applications requiring PV-based water pumping system (WPS). Originally, water was pumped using DC motors [10]. Due to the shortcomings of DC motors, including their low efficiency and frequent maintenance requirements due to the presence of brushes and commutators, AC induction motors are used for water pumping services [11], [12]. Additional classifications for synchronous motors are Trapezoidal and Sinusoidal wave permanent magnet motors, which are also referred to as BLDC motors [13], [14]. Because of the benefits, such as excellent savings, high reliability, minimal repairs, and good acceleration, BLDC motors are ideal for PV-fed WPS [15]. Numerous challenges prevent solar WPS from operating as effectively, dependably, and as they should. The irregular water flow and pressure caused by variations in sun irradiation, which lowers system efficiency, is one of the main issues. High energy usage, problems with system maintenance, and component failures all make the issue harder. In addition, expensive downtime and repairs may result from technical problems including battery deterioration, inverter or controller failure, and pumping system mechanical or electrical failure. These difficulties highlight the need for creative solutions to maximize the sustainability, dependability, and efficiency of solar WPS.

A sustainable energy source is required to carry out certain basic functions in remote locations, like water pumping. This requirement can be satisfied by renewable energy. Given the daily variations in temperature, wind speed, and humidity, weather conditions can have a negative impact on the utilization of renewable energy in these places. Utilizing various controlling schemes, such as weather forecasting, battery management, maximum power point tracking (MPPT) systems and integrating them into the WPS is the way to solve this problem. Including these elements reduces the negative consequences of temperature fluctuations by predicting sun irradiance. A framework to simulate BLDC speed regulation using a PID controller was presented by Usha et al. [16]. The BLDC Motor's speed control techniques make use of dual closed-loop speed control, wherein one loop controls the gate pulses, limits current, and governs current regulation. The other loop dealt with speed control, which was needed to achieve the required speed. The necessary speed can be entered in steps or as an integer value. The reference speed was provided as a constant that can be altered following the need to get the intended speed. Even though fuzzy has proven to be evaluated in a majority of applications, it was occasionally difficult to specify the rules for certain situations. Subramanian [17] suggested employing the dynamic power containment technique (DPCT) control to reduce quantum vibration and maintain the BLDC speed. The BLDC was operated at a constant speed using an inverter. The proposed control system was substituted with the traditional cascaded method for controlling the BLDC motor's speed and current. Subsequently, an additional immediate pay method was suggested to anticipate the change in current during the deferred period. Furthermore, the developed approach was more easily utilized to select the optimal switch state for each cycle. However, the reference design's accuracy was not guaranteed due to BLDC restrictions' fluctuation. An adaptive fractional order PID was introduced by Vanchinathan and Selvaganesan [18] for BLDC engine speed management using the Artificial Bee Colony (ABC) approach. The suggested tuning technique not only minimizes the error indices but also the time domain parameters. And also, significant to note that there are a lot of restrictions on the use of Hall Effect sensors because of component failure, low dependability, the necessity for certain mechanical mounting arrangements, and electrical noise issues. To prevent these kinds of problems, a Kalman Filter was intended to estimate the motor's speed. Higher assembly time and settling time speed performances also result in more consistent state inaccuracy.

Eltoum et al. [19] presented Fractional-Order PID dependent speed control for BLDC with Varying Speed Activity. A tweaked version of the harmony search (HS) method was created for fine-tuning FOPID controller variables. To test the motor and confirm the efficacy of the suggested controller, three distinct working circumstances are applied: no load, variable load, and variable speed. Additionally, the speed-torque characteristics revealed that when a fuzzy FOPID controller was used, the least number of oscillations occurred during the gradual reduction of load. But it takes longer for the system to settle and become steady. Suryoatmojo et al. [20] presented how to use the adaptive neuro-fuzzy inference system (ANFIS) to temporarily manage BLDC drivers. To achieve steady state inaccuracy, this suggested strategy also moves forward with shorter intervals. In comparison to the other controllers, the ANFIS controller has a higher starting current and torque, but it takes less time to reach the steady state condition. The torque was a function of the current flowing through it. The torque was higher the bigger the current. Rise time is decreased and the model is created more quickly with the aid of the suggested ANFIS. However, when control rule situations were taken into account, differential controller behavior results in inferior outcomes sooner. A whale optimization algorithm (WOA) based sliding mode controller (SMC) has been presented for PV Based WPS which was described by Malla et al. [21]. In both PSC and normal conditions, the hybrid

WOA-SMC method efficiently extracts the maximum PV power. By combining the algorithm with the inverter's SMC, the inverter also functions as an MPPT for PV to lower the system's cost. Therefore, additional dc-dc converters won't be needed for MPPT. However, because the output produced by the PV modules exceeds the BLDC standard, the experimental test has been carried out in lower light. Efficiency Improvement of PV-WPS Based on BLDC Motor under PSC has been proven by Ammar *et al.* [22]. The goal of this work was to enhance a battery-free PV pumping system's power extraction capability. To achieve MPPT, a DC–DC converter has been utilized. Additionally, the BLDC motor was employed to improve the pumping system's dependability and to make the most of the power that the PV array delivers. Additionally, an MPPT method has been devised to enhance control performance in partial shade settings.

Qasimand and Atyia [23] presented a voltage source inverter (VSI) which was designed and used for solar water pump control. In order to construct effective and dependable systems that promote environmental sustainability and rural development, the scheme tackles operational disparities and efficiency challenges. The submersible pump speed is determined by the P&O MPPT technique that depends on the PV panel's power. There was no need for location or speed sensors when using the sensorless speed control method. In the absence of mechanical speed sensors, the black electro-motives force (BEMF) determines speed by estimating the flux angle. By processing with the need for pricey and complex speed sensors, this technique lowers expenses and streamlines the system. While moderated, the torque and current harmonics was still there. An analysis of electrical configuration topologies for improving the efficiency of solar photovoltaic water pumping systems (SPVWPS) has been shown by Chadge *et al.* [24]. The increasing importance of SPVWPS as a feasible choice for producing power in isolated, remote, and non-electrified areas serves as what motivates the research. These places, which frequently exist in underdeveloped countries like India, lack access to traditional electrical sources. The main goal of this research was to support the development of water supply systems for residential usage and livestock drinking in remote places. Water extraction using SPVWPS has been viewed as a potential substitute in places without access to traditional power sources. However, accurate knowledge and practical competence regarding system sizing and installation are necessary for the widespread application of SPVWPS. The design, modeling, and computation of a variable frequency drive (VFD) with LC filter for a water pump have been proven by Kapp *et al.* [25]. The three-phase inverter's design depends on a PWM generator, which was created by a different PWM generator subsystem. Both with and without an LC filter, circuit and voltage signal testing was carried out. The voltage to frequency ratio (V/F), that serves as the foundation for control system formulation and computation has been designed to maintain motor speed stability as frequency shifts from 30 Hz to 50 Hz. If the average daily sunbathing hours exceeded 100% and were insufficient to supply 50 Hz, the system could move up a minimum of 90% extra water. The above-stated literature study addresses different algorithms and control schemes for maximizing the efficiency of submersible BLDC motors in solar-powered water pump systems. The primary challenges to maximizing BLDC motor performance in solar-powered WPS systems are oscillations, sensor malfunctions, and partial shading. The conventional algorithm's has inability to track the maximum power point in partial shade condition which reduced the efficiency results. Hall sensors also produces several challenges because of component failure, low dependability, and problems with electrical noise. Furthermore, managing BLDC motors requires finding a balance between multiple objectives including adaptability, dependability, and efficiency. In order to maximize performance, the system's complexity requires advanced control techniques and algorithms, therefore innovative techniques must be developed to get over these challenges and guarantee the effective and long-term operation of solar-powered WPS. Therefore, this research proposed IMO-MP&O to enhance the efficiency, reliability, and performance of solar-powered WPS using BLDC motors.

The major contribution of this work is as follows,

− Here, a bidirectional converter with IMO-MP&O is proposed to regulate the voltage level of the BLDC motor at different irradiation conditions. Further, it is intended to modify the duty cycle for controlling the output voltage of the converter.
− Also, a sensorless control strategy is used to enhance the system efficiency by minimizing the dependability on hall sensors.
− Moreover, MATLAB/Simulink is used to analyze the performance parameters of the IMO-MP&O on submersible BLDC motor.

The organization of this research is mentioned as follows: Section 2 explains the process and modelling of BLDC motor. Section 3 provides the description about proposed IMO-MP&O method. Section 4 demonstrates the result analysis and its comparison. Finally, section 5 states the conclusion of this study.

2. PROPOSED METHOD

Figure 1 depicts an overall block diagram that contains multi-stage solar PV-WPS with several power-electronic components. The water is kept in tanks, which serve as storage and organize with the need for batteries well to save from a few dependable requirements. PV arrays are made up of a series-parallel arrangement of PV modules that are connected following the voltage requirements. The PV output power fluctuates according to changes in irradiation. Thus, PV array ought to be run at its maximum power taking temperature, or MPPT.

The synchronous motor is powered by the DC-DC converter's output, which is received by the three-phase VSI. When selecting solar water pumps, the pumping head and daily water requirement should be taken into account. Water pumping applications are where submersible pumps are most frequently used [26]. Direct current power generation from solar energy is facilitated by the p-n junction in solar cells. There are two variants of the PV model's comparable circuit: single diode and double diode. It is recommended that analytical research and design be conducted using single diodes. Location, operating conditions, and rising temperatures all have a big impact on PV power. By connecting the solar modules in either parallel or series, one may ascertain the voltage and capacity of PV which raises the MPP. The PV cell's V-I characteristic is revealed in Figure 2.
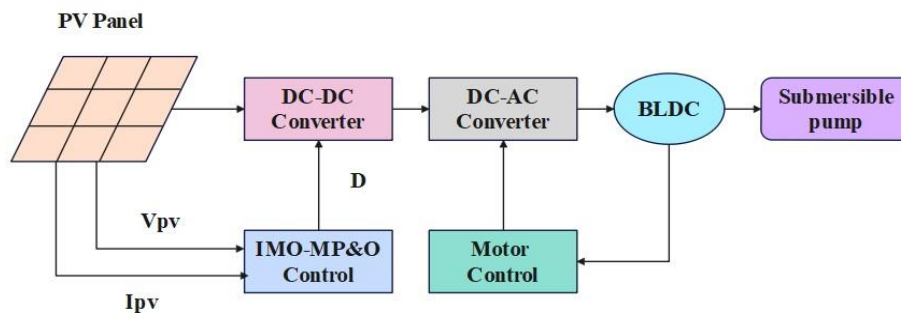

Figure 1. Overall block diagram for the proposed model
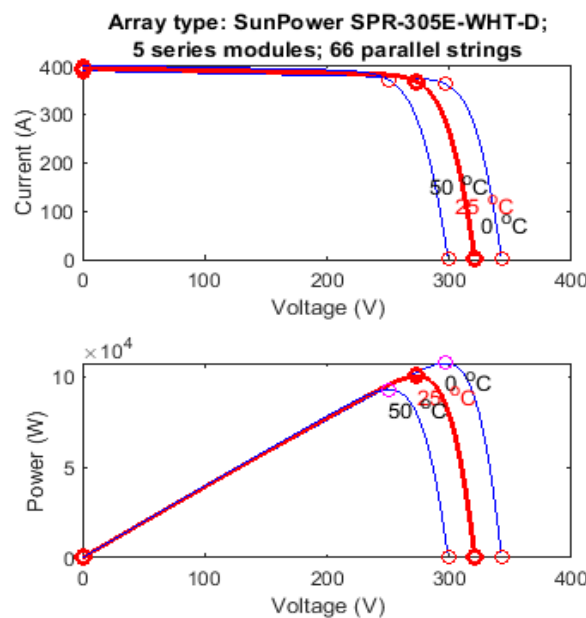

Figure 2. V-I properties of PV cell

In (1) is utilized to detect the output power,

$$P_{MPPT}(t) = I_{MPPT}(t) \times V_{MPPT}(t) \tag{1}$$

the current and voltage are declared in (2) and (3).

$$I_{MPPT}(t) = I_{SC}\left\{1 - C_1\left[exp\left(\frac{V_M}{C_2 \times V_{OC}}\right)\right]\right\} + \Delta I(t) \tag{2}$$

$$V_{MPPT}(t) = V_M + \mu V_{OC}.\Delta T(t) \tag{3}$$

$V_{OC} \& I_{SC}$ is signified as open circuit voltage and short circuit current; Capacitances are stated as C_1 and C_2; V_M is represented as maximum voltage which are represented in (4)-(7) accordingly. Where, I_M is stated as maximum current; $T_{c,ref}$ stated as cell temperature; $GT(t)$ stated as the level of irradiation.

$$C_1 = \left(1 - \frac{I_M}{I_{SC}}\right) \times exp\left(-\frac{V_M}{C_2 \times V_{OC}}\right) \tag{4}$$

$$C_2 = \left(\frac{V_M}{V_{OC}} - 1\right) \times \left[ln\left(1 - \frac{I_M}{I_{SC}}\right)\right]^{-1} \tag{5}$$

$$\Delta I(t) = I_{SC}\left(\frac{GT(t)}{G_{ref}} - 1\right) + \alpha_{1,sc} \times \Delta T(t) \tag{6}$$

$$\Delta T(t) = T_c(t) - T_{c,ref} \tag{7}$$

The self-inductance and stator resistance of each winding are assumed to be equal in the BLDC model. In (8) provides a matrix expression for the armature of DC machines. This equation is similar to the stator phase voltage equation of BLDC motors.

$$\begin{bmatrix} V_a \\ V_b \\ V_c \end{bmatrix} = R\begin{bmatrix} 1 & 0 & 0 \\ 0 & 1 & 0 \\ 0 & 0 & 1 \end{bmatrix}\begin{bmatrix} i_a \\ i_b \\ i_c \end{bmatrix} + \begin{bmatrix} L-M & 0 & 0 \\ 0 & L-M & 0 \\ 0 & 0 & L-M \end{bmatrix}\frac{d}{dt}\begin{bmatrix} i_a \\ i_b \\ i_c \end{bmatrix} + \begin{bmatrix} E_a \\ E_b \\ E_c \end{bmatrix} \tag{8}$$

R_a, R_b and R_c denote the terminal resistances; V_a, V_b and V_c represent the stator phase voltages. i_a, i_b and i_c refers to motor input currents; E_a, E_b and E_c refers trapezoidal back emf. The torque of BLDC is assessed by (9):

$$T_e = \frac{P}{w_m} \tag{9}$$

where, $P = E_a i_a + E_b i_b + E_c i_c$. In (10) is employed to predict the torque in the synchronously rotating frames:

$$T_e = \frac{3}{2}\frac{p_n}{2}\left[\left(\frac{dL_d}{d\theta_e}i_{sd} + \frac{d\varphi_{rd}}{d\theta_e} - \varphi_{sq}\right)i_{sd} + \left(\frac{dL_q}{d\theta_e}i_{sq} + \frac{d\varphi_{rq}}{d\theta_e} - \varphi_{sd}\right)i_{sq}\right] \tag{10}$$

where, $\varphi_{sq} = L_q i_{sq} + \varphi_{rq}$ and $\varphi_{sd} = L_d i_{sd} + \varphi_{rd}$. p_n refers the number of poles; θ_r characterizes the rotor angle; φ_{rd}, φ_{rq}, φ_{sd} and φ_{sq} refers the rotor and stator flux linkages.

3. MAYFLY OPTIMIZATION

Users of the IMO determine the duty cycle of the converter; the output of the IMO is the control signal, which is a gauge of the efficiency of the fertility rate. Because the male mayflies are consistently stronger, they will likewise perform better in terms of augmentation. The MO approach [27] modifies the positions of the variables based on their current positions $p_i(t)$ with the same settings as the optimization algorithms and velocity $v_i(t)$ at the current iteration. In (11) is used to change the placements of every mayfly. On the other hand, its velocity could experience some changes.

$$p_i(t+1) = p_i(t) + v_i(t+1) \tag{11}$$

3.1. Process of MO in terms of stages

The process of MO algorithms contains the male mayfly movement, female mayfly movement and its mating which are explained as follows.

3.1.1. Movements of male mayflies

The velocity is updated by original fitness $f(x_i)$ and best fitness in earlier movements $f(x_{h_i})$. IF $f(x_i) > f(x_{h_i})$, the earlier ideal movements are stated in (12), where g is declared as a variable; α_1, α_2 and β are mentioned as stable. The Cartesian spacing is mentioned as γ_p and γ_g that is declared in (13).

$$v_i(t+1) = g.v_i(t) + \alpha_1 e^{-\beta\gamma_p^2}[x_{h_i} - x_i(t)] + \alpha_2 e^{-\beta\gamma_g^2}[x_g - x_i(t)] \tag{12}$$

$$\|x_i - x_j\| = \sqrt{\sum_{k=1}^{n}(x_{ik} - x_{jk})^2} \tag{13}$$

3.1.2. Female mayfly's motion

Mayflies were able to distinguish themselves via subtle movements. MO approach supposed that the most fit male and female mayflies had to mate first. The other male and female may have bred similarly. Therefore, IF $f(y_i) < f(x_i)$, in (14) is written as,

$$v_i(t+1) = g.v_i(t) + \alpha_3 e^{-\beta\gamma_{mf}^2}[x_i(t) - y_i(t)] \tag{14}$$

α_3 is acknowledged as an alternative constant. Cartesian distance is stated as γ_m.

3.1.3. Mating of mayflies

The upper half of the mayflies are capable of mating and producing two or more offspring. The manner expressed in (15) and (16) suggests that the rate at which their progeny separate from their moms is random. Where Gauss distribution is stated as L.

$$offspring1 = L \times male + (1 - L) \times female \tag{15}$$

$$offspring1 = L \times female + (1 - L) \times male \tag{16}$$

3.2. Process of improved mayfly optimization

Members of a swarm randomly alter their velocities under certain conditions, as shown by (13) and (15), which support this [28]. In (17) shows that with extra context, the adjusted distance's parts appear as below. To accommodate some situations, in (17) should be improved, as revealed in subsequent (18).

$$v_p = \alpha_i e^{-\beta\gamma_j^2}(p_j - p_i) \tag{17}$$

$$v_p = \alpha_i e^{-\frac{\beta}{\gamma_j}}(p_j - p_i) \tag{18}$$

MPPT accuracy is ensured by the hybrid IMO-MP&O algorithm's flexibility in responding to shifting environmental factors like partial shading. The parameters of the algorithm are capable of being adjusted to accommodate various PV panel setups and climatic circumstances. A rational and theoretically strong method for maximizing the efficiency and dependability of solar-powered WPS is provided by the Hybrid IMO-MP&O algorithm. For practical WPS applications, this methodology offers a reliable, effective and scalable solution by combining the advantages of IMO-MP&O.

3.3. Sensorless control scheme

Additionally, sensorless Control saves maintenance requirements, boosts dependability, and simplifies the system by doing away with hall sensors. The suggested Hybrid IMO-MP&O algorithm improves the overall efficiency, dependability, and maintainability of solar-powered WPS by implementing sensorless control. The control block diagram of a zero crossing-based back-EMF Submersible BLDC motor with sensorless control is suggested in this research. The motor's line voltages are detected by three voltage sensors. A straightforward resistive divider circuit is used to scale down the observed input line voltages before feeding them into the digital signal controller's analog-to-digital converter. The line voltage differences are then computed. The current traveling through the winding does not instantly stop because of the motor inductance; instead, it travels in a different direction through the freewheeling diodes [29].

As a result, back-EMF zero-crossing instants are falsely detected. Here, a low-pass filter (LPF) is employed in the suggested control scheme to filter the voltage spikes caused by the conduction of the freewheeling diode. This is done using a sample and hold circuit. There are two benefits to employing an

LPF. First, it removes the higher frequency voltage components from the pulse width modulation (PWM) operation as well as the voltage spikes caused by diode conduction. Second, the necessary phase shift for driving the currents following the zero-crossing detection can be achieved by designing the filter's cut-off frequency. When the rotor is stationary and its position is unknown, the back-EMF is initially zero. Therefore, by stimulating any two phases of the BLDC motor, the rotor is prepositioned [30]. Afterward, a phase commutation start-up procedure is used until the motor produces a sufficient back-EMF for submersible BLDC motor. Figure 3 shows the flow diagram for sensorless control of submersible motor.
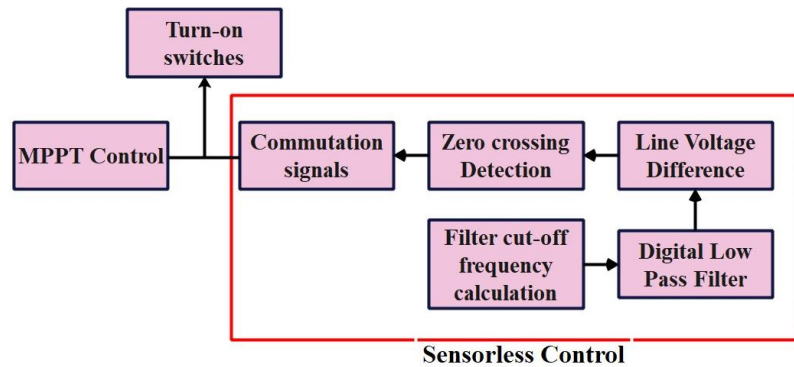
Figure 3. Flow diagram for sensorless control of submersible motor

3.4. Modified perturb and observe

It is anticipated that MP&O will address the drift issue by incorporating the current and voltage variation data (ΔI and ΔV). To solve the drift issue, ΔI and ΔV circuits are added to the MP&O. The MPPT can find the MPP even in total shade since MP&O can overcome the constraints of a few peaks by adjusting the step value. When MP&O reaches its maximum value, power loss and instability stop decreasing [31]. Consequently, there are fewer fluctuations and a quicker time to reach the optimal functioning occasion. The main difference among P&O-MP&O is the drifting problem, which is resolved in this optimization by varying the voltage and current. If the irradiance is higher, MP&O observe dP, dV and dI asnull and hence, duty cycle is developed through ΔDn that is stated as variable step size which is represented in (19).

$$\Delta Dn = \pm M|\Delta G| \tag{19}$$

Where a shift in incidence is defined as ΔG and a fixed restriction is specified as M. Numerous cost-effective and scientifically sound approaches already exist for creating a hybrid energy system [32]. Using the following methods, this procedure can be carried out until the PV system under PSC achieves the global optimum position for Vmpp.

4. RESULTS AND DISCUSSION

Using the suggested IMO-MP&O, the Simulink example for BLDC motor speed control is verified using MATLAB software. To validate this simulated model, an Intel (R) Core i3 computer chip running at 2.53 GHz, 8 GB RAM, and 64-bit OS are also required. This paper proposes the IMO-MP&O approach for BLDC engine speed management. The equivalent model is used to calculate the current produced by the PV, and Table 1 lists the parameters of BLDC motors and PV arrays.

The suggested system offers significant advantages such as enhanced resilience and ease of control, allowing for technique modifications. According to the IMO-MP&O simulation findings using MATLAB to control the motor speed, the desired speed is attained with a faster response time as compared to conventional controllers. The dynamic characteristics of BLDC are obtained, and analysis reveals that the suggested approach is incredibly effective in controlling the BLDC motor via a wide speed limit. The speed controller is used separately from the IMO-MP&O. Values for error ratio, settling time, and speed are used in the performance analysis. Figure 4 shows how the BLDC engine is controlled using IMO-MP&O.

Table 1. Specification of overall setting parameters

Parameters	Value
Maximum power (Pmax)	335 (0-3%)
Maximum voltage (Vmp)	39.24 V
Tolerance for Voc & Isc	5%
Maximum current (Imp)	8.54 A
Maximum system voltage	1500VDC
Maximum series fuse	A
Application class	15A
Protection again at electrical shock	II
Module size	$1985 \times 1000 \times 35$ mm
Module weight	22 kg
Fill factor	79.07%
Amplitude	220 V
Module efficiency	16.88%
Power	3 hp
Frequency	60 Hz
Stator inductance Ls (H)	8.5e-3
Speed	1650 rpm
Voltage	300 Vdc
Flux linkage (V.s)	0.175
Stator resistance Rs (ohm)	0.2
Inertia, viscous damping, pole pairs, static friction [J (kg.m2) F (N.m.s) p () Tf (N.m)]	[0.089,0.005,4]
Back EMF flat area (degree)	120
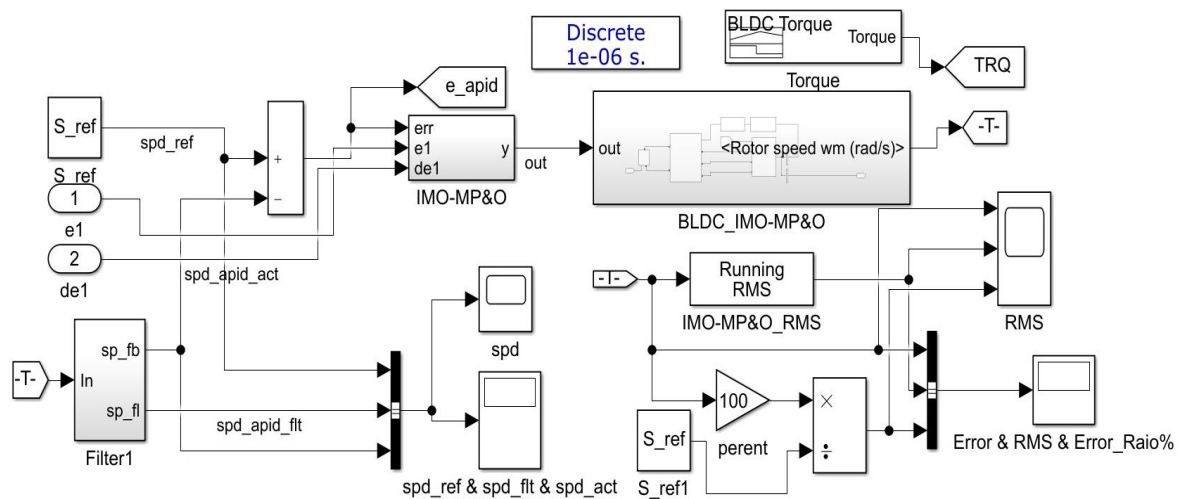
Figure 4. MATLAB design of proposed methodology

4.1. Performance analysis of PV

It would be interesting to enhance this system by adding a few features to the voltage source inverter, such as active power filtering and power factor adjustment. Current harmonics from nonlinear loads connected to the grid degrade the mains power quality. This armature current can be compensated for with active power filters. If PV is linked to the grid, voltage regulation issues might come up. However, increasing voltage within the network can lead to levels exceeding the permitted bandwidth of 5%. The intermittent nature of photovoltaics makes voltage variations common as well. This might cause voltage fluctuations in addition to frequently tampering with voltage regulators carrying them out. The MPPT efficiency figures and MPP power outcomes are shown in Table 2. Table 2 unequivocally demonstrates that the recommended IMO-MP&O attains a higher degree of efficiency (99.58%) than the current techniques.

Table 2. Comparative analysis of the proposed method

Techniques	Obtained MPP power (W)	Efficiency (%)
MO-P&O	259.75	87.31
IMO-P&O	286.34	92.37
IMO-MP&O	302.57	99.58

To get the PV to operate at the MPPT, a boost converter is used. In such cases, a change in load will alter the duty cycle of the boost converter. As a result, load current could change in the event of a load increment/decrement which directs the PV to a new MPPT point. Consequently, the connected load will determine how the MPPT value changes.

4.2. Voltage and current in MPPT

The MPPT measures are displayed in Figures 5 and 6. The results show that, in terms of MPPT efficiency, IMO-MP&O performs better than the conventional techniques. As illustrated in Figures 5 and 6, IMO-MP&O provides improved efficacy in both constant and dynamic phases. IMO-MP&O's current switching between variable and steady modes makes it operate more effectively. The WPS powered by a BLDC motor and supplied by solar operate more efficiently due to the IMO-MP&O algorithm. The suggested approach successfully monitors the motor speed above the minimally necessary speed and track the maximum power point.
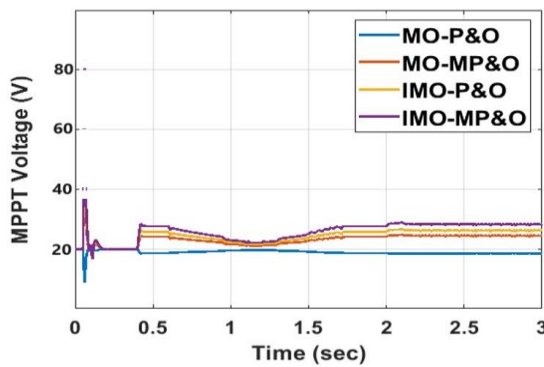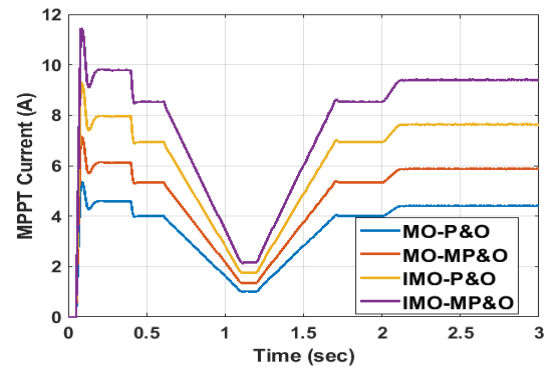

Figure 5. Voltage at MPPT

Figure 6. Current at MPPT

4.3. Performance of BLDC motor

The reference speed and predicted speed error are used to relate the BLDC motor speed, which is taken as feedback. The anticipated speed error and change in speed error are expected to be in the direction of the proposed IMO-MP&O, with the reference speed value being 1650 rpm. Figure 7 shows the error proportion upsides of the BLDC engine. The BLDC engine's assessed speed is displayed in Figure 8. Sensors, such as position-detecting control sensors, are used to operate BLDC engines. It must be feasible to control the speed using standard PID and PI regulators. BLDC engines are important for a variety of applications.

Furthermore, at higher speeds, the torque ripple becomes uncontrollable. Thus, even with the best ripple elimination technique, no increase in efficiency is seen at higher speeds. Within the specified speed range, an improvement in efficiency is noted because the torque ripple is eliminated only at lower speeds. While compared to an induction or brushed DC motor, the presented BLDC motor delivers a good amount of water even at low speeds because of its high efficiency. Figure 8 shows the measured torque of the BLDC engine. BLDC engines are operated by sensors, such as position-detecting control sensors. The speed must be manageable with conventional PID and PI regulators. BLDC engines are crucial for many different uses.
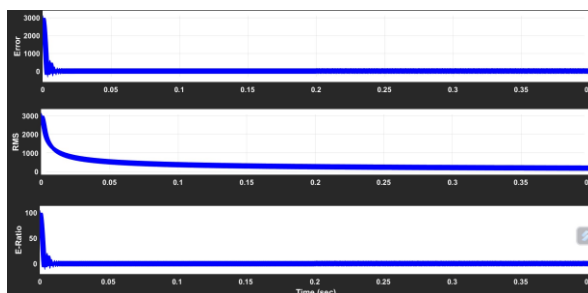

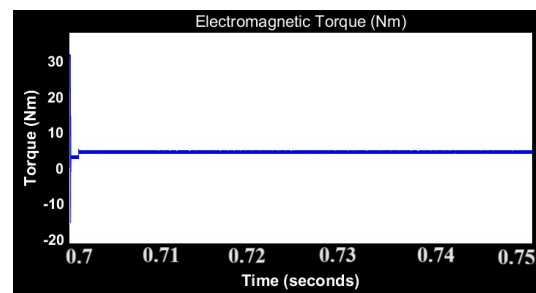Figure 7. Error ratio values for BLDC motor

Figure 8. Torque for BLDC motor

The PV array's maximum power available controls the speed. Any change in the atmospheric conditions affects the PV array's power output, which in turn affects the BLDC motor's speed. The BLDC motor in the solar PV fed WPS is intended to be operated at a speed higher than 1100 rpm, (i.e.) the minimum speed needed to pump the water. The BLDC engine's assessed speed is displayed in Figure 9. Therefore, the usage of LPF removes the diode-caused voltage spikes, filters the PWM-caused harmonic components, and provides an adequate delay following the zero-crossing instant. Because of this, the motor is successfully commutated by the virtual hall signals produced by the sensorless algorithm until it reaches its rated speed.
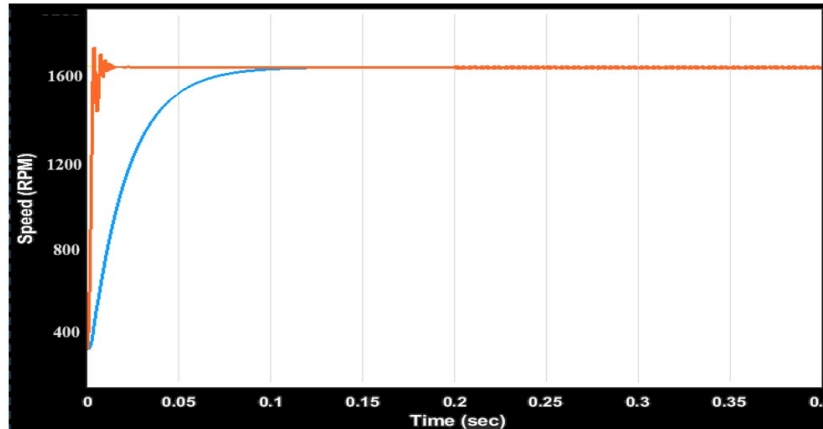

Figure 9. Speed for BLDC motor

4.4. Comparative analysis

This method guarantees optimal performance and dependability by tracking the MPP and maintaining the motor speed. Several approximations are made to evaluate the BLDC engine and MPPT efficiency. Table 3 shows the comparative analysis of MPPT efficiency with the existing P&O-MPPT [23]. The comparison is made under different irradiation values which are shown in Table 3.

Table 3 makes it evident that the existing P&O-MPPT [23] is achieved less efficiency than proposed IMO-MP&O with respect to different irradiations. While the existing P&O-MPPT [23] has obtained an efficiency of 99.4%, but the proposed IMO-MP&O has accomplished a higher efficiency of 99.58%. Table 4 shows the comparative analysis of pump efficiency with existing SPVWPS [24].

From the Table 4, it clearly shows that proposed IMO-MP&O accomplished higher pump efficiency and average pump efficiency of 79.64% and 70.39% respectively. While the existing SPVWPS [24] has obtained an efficiency of 74.59% and 63.87% respectively. The findings demonstrate that the concept via the IMO-MP&O exceeds the current approach in all the patterns.

Table 3. Comparison of MPPT efficiency

Irradiation	Efficiency (%)	
	P&O-MPPT [23]	Proposed IMO-MP&O
920	N/A	99.58
843	N/A	99.52
367	N/A	99.46
313	99.3	99.41
263	99.2	99.33
223	98.9	99.24
183	98.2	99.12
112	99.4	99.41
88	99.1	99.22
56	98.4	98.89

Table 4. Comparison of pump efficiency

Pattern	Pump efficiency (%)		Average pump efficiency (%)	
	SPVWPS [24]	Proposed IMO-MP&O	SPVWPS [24]	Proposed IMO-MP&O
6S*2P	74.59	79.64	63.87	70.39
5S*2P	69.55	76.28	60.77	68.72
4S*2P	72.46	75.71	58.43	66.94

4.5. Discussion

The aim of this work is to develop an efficient, consistent, and maintenance-free solution for solar WPS application. Therefore, it combines an improved mayfly optimization (IMO) and Modified P&O (MP&O) for extracting the maximum power to obtain higher efficiency. Further, a sensorless control strategy is used to minimize the hall sensors requirement to expand the system's reliability. For the analysis purpose, the proposed IMO-MP&O is compared with existing P&O-MPPT [23] and SPVWPS [24] respectively under different irradiation condition. From the outcomes, it evidently displays that IMO-MP&O accomplished higher efficiency of 99.58% over existing P&O MPPT [23] which has the maximum efficiency of 99.3%. While analyzing in terms of pump efficiency, the proposed IMO-MP&O accomplished higher value of 79.64%, 76.28% and 75.71% under 6S*2P, 5S*2P, and 4S*2P respectively, that is better when compared with existing SPVWPS [24] which has 74.59%, 69.55% and 72.46% respectively. Whereas in terms of average pump efficiency, the proposed IMO-MP&O attained higher value of 70.39%, 68.72% and 66.94% under 6S*2P, 5S*2P, and 4S*2P respectively; where the existing SPVWPS [24] has 63.87%, 60.77% and 58.43% respectively.

This study addresses the shortcomings of existing algorithms such as P&O-MPPT [23] and SPVWPS [24] by providing an innovative approach to MPPT under PSC in comparison to earlier studies. Whereas the previous research has concentrated on improving individual parts, for example, in P&O-MPPT [23], the sensorless speed control method lowers harmonics, certain residual torque and current harmonics remain, but still, it has an impact on the system durability and performance. Similarly, in SPVWPS [24], During the periods of low solar irradiance, poor efficiency and dependability could arise from the absence of energy storage solutions for SPVWPS. But this hybrid algorithm (IMO-MP&O) reduces the impact of shading, noise and environmental factors to provide better results. Even, this IMO-MP&O has some limitations, for example, still, more research is needed to fully understand the computational complexity and sensitivity to changing parameters.

The proposed IMO-MP&O has obtained strong performance in a range of partial shading conditions which highlighting its potential for real-world applications. Developing an effective MPPT algorithm for solar-powered WPS under PSC was the goal of this study while addressing the difficulties associated with sustainable WPS. The findings highlight how crucial it is to maximize energy extraction in solar-powered systems, especially when there is partial shade. Even though this study makes a substantial contribution to the field, there are still issues that need to be resolved, like how scalable the technique is for large-scale WPS. Further research needs to concentrate on resolving these constraints and investigating the possibilities of hybrid algorithms for other renewable energy uses.

5.   CONCLUSION

This research exploited hybrid IMO-MP&O algorithm as a basis for its MPPT approach to ensure that the operation of WPS is at maximum power under PSC. Subsequently, the hybrid IMO-MP&O algorithm incorporates a position sensorless control technique to better improve system reliability. This strategy is contrasted with the existing procedures for PV system MPPT performance monitoring under PSC. The suggested algorithm maximizes energy extraction, lowers servicing requirements and assures continuous functioning. Further, it has been found that IMO-MP&O algorithm increases the amount of energy that can be extracted from the PV system. From the evaluation, it evidently displays that hybrid IMO-MP&O obtained an efficiency of 99.58% which is superior over existing methods. Even though, the suggested IMO-MP&O algorithm are computationally complex and requiring significant processing power. Furthermore, the performance of the algorithm is sensitive to parameter modification and requiring specialized knowledge. Moreover, it might not be appropriate for large solar-powered WPS systems. Therefore, this work will investigate the alternatives to optimization algorithms in the future and create advanced control schemes to increase the system performances in the research field. Further, the efficient solar-powered WPS can confirm the consistent water supply, supporting agriculture and manufacturing in the community.

REFERENCES

[1]   A. W. Lins and R. Krishnakumar, "Tuning of PID controller for a PV-fed BLDC motor using PSO and TLBO algorithm," *Applied Nanoscience (Switzerland)*, vol. 13, no. 4, pp. 2911–2934, Feb. 2023, doi: 10.1007/s13204-021-02272-x.

[2]   M. S. N. Krishna konijeti and M. L. Bharathi, "Extraction of maximum power from solar with BLDC motor driven electric vehicles based HHO algorithm," *Advances in Engineering Software*, vol. 170, p. 103137, Aug. 2022, doi: 10.1016/j.advengsoft.2022.103137.

[3]   K. Vanchinathan, K. R. Valluvan, C. Gnanavel, and C. Gokul, "Numerical simulation and experimental verification of fractional-order PIλ controller for solar PV fed sensorless brushless DC motor using whale optimization algorithm," *Electric Power Components and Systems*, vol. 50, no. 1–2, pp. 64–80, Jan. 2022, doi: 10.1080/15325008.2022.2135644.

[4]   P. Jena, R. Pudur, P. K. Ray, and A. Mohanty, "ANN based MPPT applied to solar powered water pumping system using BLDC motor," in *1st IEEE International Conference on Sustainable Energy Technologies and Systems, ICSETS 2019*, Feb. 2019, pp. 200–205, doi: 10.1109/ICSETS.2019.8744804.

[5] K. Y. Yap, H. H. Chin, and J. J. Klemeš, "Solar energy-powered battery electric vehicle charging stations: Current development and future prospect review," *Renewable and Sustainable Energy Reviews*, vol. 169, p. 112862, Nov. 2022, doi: 10.1016/j.rser.2022.112862.

[6] M. Nivas, R. K. P. R. Naidu, D. P. Mishra, and S. R. Salkuti, "Modeling and analysis of solar-powered electric vehicles," *International Journal of Power Electronics and Drive Systems*, vol. 13, no. 1, pp. 480–487, Mar. 2022, doi: 10.11591/ijpeds.v13.i1.pp480-487.

[7] Z. M. S. Elbarbary, A. A. Alaifi, S. F. Alqahtani, I. M. Shaik, S. K. Gupta, and V. Gali, "Design and analysis of high-gain DC–DC chopper topologies for PV-fed BLDC motor drive system," *Frontiers in Engineering and Built Environment*, vol. 4, no. 1, pp. 29–43, Jul. 2024, doi: 10.1108/febe-09-2022-0038.

[8] H. Alrajoubi and S. Oncu, "A golden section search assisted incremental conductance MPPT control for PV fed water pump," *International Journal of Renewable Energy Research*, vol. 12, no. 3, pp. 1628–1636, 2022, doi: 10.20508/ijrer.v12i3.13119.g8549.

[9] K. S. Kavin and P. Subha Karuvelam, "PV-based grid interactive PMBLDC electric vehicle with high gain interleaved DC-DC SEPIC converter," *IETE Journal of Research*, vol. 69, no. 7, pp. 4791–4805, Aug. 2023, doi: 10.1080/03772063.2021.1958070.

[10] D. Mohanraj *et al.*, "A review of BLDC motor: state of art, advanced control techniques, and applications," *IEEE Access*, vol. 10, pp. 54833–54869, 2022, doi: 10.1109/ACCESS.2022.3175011.

[11] A. Sen and B. Singh, "Parametric observer controlled motor invariant electronic commutation of photovoltaic powered BLDCM without position sensor," *IEEE Transactions on Power Electronics*, vol. 38, no. 9, pp. 11304–11314, Sep. 2023, doi: 10.1109/TPEL.2023.3282449.

[12] S. Amose Dinakaran, A. Bhuvanesh, A. S. Kamaraja, P. Anitha, K. Karthik Kumar, and P. Nirmal Kumar, "Modelling and performance analysis of improved incremental conductance MPPT technique for water pumping system," *Measurement: Sensors*, vol. 30, p. 100895, Dec. 2023, doi: 10.1016/j.measen.2023.100895.

[13] P. Van Minh, T. D. Chuyen, D. Q. Du, and H. D. Co, "Development of position tracking electric drive system to control BLDC motor working in very low mode for industrial machine application," *International Journal of Power Electronics and Drive Systems*, vol. 14, no. 2, pp. 688–697, Jun. 2023, doi: 10.11591/ijpeds.v14.i2.pp688-697.

[14] B. Ramesh, K. Chenchireddy, B. N. Reddy, B. Siddharth, C. V. Kumar, and P. Manojkumar, "Closed-loop control of BLDC motor using hall effect sensors," *International Journal of Applied Power Engineering*, vol. 12, no. 3, pp. 247–254, 2023, doi: 10.11591/ijape.v12.i3.pp247-254.

[15] A. K. Gautam, M. Tariq, K. S. Verma, and J. P. Pandey, "An intelligent BWO algorithm-based maximum power extraction from solar-PV-powered BLDC motor-driven light electric vehicles," *Journal of Intelligent and Fuzzy Systems*, vol. 42, no. 2, pp. 767–777, Jan. 2022, doi: 10.3233/JIFS-189747.

[16] S. Usha, P. M. Dubey, R. Ramya, and M. V. Suganyadevi, "Performance enhancement of bldc motor using pid controller," *International Journal of Power Electronics and Drive Systems*, vol. 12, no. 3, 1335–1344, Sep. 2021, doi: 10.11591/ijpeds.v12.i3.pp1335-1344.

[17] S. Subramanian, R. Mohan, S. K. Shanmugam, N. Bacanin, M. Zivkovic, and I. Strumberger, "Speed control and quantum vibration reduction of brushless DC motor using FPGA based dynamic power containment technique," *Journal of Ambient Intelligence and Humanized Computing*, Feb. 2021, doi: 10.1007/s12652-021-02969-5.

[18] K. Vanchinathan and N. Selvaganesan, "Adaptive fractional order PID controller tuning for brushless DC motor using artificial bee colony algorithm," *Results in Control and Optimization*, vol. 4, p. 100032, Sep. 2021, doi: 10.1016/j.rico.2021.100032.

[19] M. A. M. Eltoum, A. Hussein, and M. A. Abido, "Hybrid fuzzy fractional-order PID-based speed control for brushless DC motor," *Arabian Journal for Science and Engineering*, vol. 46, no. 10, pp. 9423–9435, Jan. 2021, doi: 10.1007/s13369-020-05262-3.

[20] H. Suryoatmojo, D. R. Pratomo, M. R. Soedibyo, D. C. Riawan, E. Setijadi, and R. Mardiyanto, "Robust speed control of brushless dc motor based on adaptive neuro fuzzy inference system for electric motorcycle application," *International Journal of Innovative Computing Information and Control*, vol. 16, no. 2, pp. 415–428, 2020.

[21] S. G. Malla *et al.*, "Whale optimization algorithm for PV based water pumping system driven by BLDC motor using sliding mode controller," *IEEE Journal of Emerging and Selected Topics in Power Electronics*, vol. 10, no. 4, pp. 4832–4844, Aug. 2022, doi: 10.1109/JESTPE.2022.3150008.

[22] A. Ammar, K. Hamraoui, M. Belguellaoui, and A. Kheldoun, "Performance enhancement of photovoltaic water pumping system based on BLDC motor under partial shading condition †," in *Engineering Proceedings*, Feb. 2022, vol. 14, no. 1, p. 22, doi: 10.3390/engproc2022014022.

[23] M. A. Qasim and T. H. Atyia, "Design and implementation of VSI for solar water pump control," *Tikrit Journal of Engineering Sciences*, vol. 31, no. 1, pp. 193–210, Mar. 2024, doi: 10.25130/tjes.31.1.17.

[24] R. Chadge *et al.*, "Investigation of electrical configuration topologies for enhancing the performance of solar photovoltaic water pumping system," *Electric Power Components and Systems*, pp. 1–16, Feb. 2024, doi: 10.1080/15325008.2024.2319312.

[25] S. Kapp, C. Wang, M. McNelly, X. Romeiko, and J. K. Choi, "A comprehensive analysis of the energy, economic, and environmental impacts of industrial variable frequency drives," *Journal of Cleaner Production*, vol. 434, p. 140474, Jan. 2024, doi: 10.1016/j.jclepro.2023.140474.

[26] B. N. Kar, P. Samuel, A. Mallick, and J. K. Pradhan, "Grid-connected solar PV fed BLDC motor drive for water pumping system," *Distributed Generation and Alternative Energy Journal*, vol. 38, no. 5, pp. 1477–1504, Jul. 2023, doi: 10.13052/dgaej2156-3306.3856.

[27] S. Mo, Q. Ye, K. Jiang, X. Mo, and G. Shen, "An improved MPPT method for photovoltaic systems based on mayfly optimization algorithm," *Energy Reports*, vol. 8, pp. 141–150, Aug. 2022, doi: 10.1016/j.egyr.2022.02.160.

[28] G. Lei, X. Chang, Y. Tianhang, and W. Tuerxun, "An improved mayfly optimization algorithm based on median position and its application in the optimization of PID parameters of hydro-turbine governor," *IEEE Access*, vol. 10, pp. 36335–36349, 2022, doi: 10.1109/ACCESS.2022.3160714.

[29] K. Joshi, V. Raut, S. Waghmare, M. Waje, and R. Patil, "Maximum power operation of a PV system employing zeta converter with modified P&O algorithm," *International Journal of Engineering Trends and Technology*, vol. 70, no. 7, pp. 348–354, Jul. 2022, doi: 10.14445/22315381/IJETT-V70I7P236.

[30] M. Mounira and C. Djamila, "A new approach of robust speed-sensorless control of doubly fed induction motor fed by photovoltaic solar panel," *International Journal of Power Electronics and Drive Systems*, vol. 14, no. 1, pp. 153–166, Mar. 2023, doi: 10.11591/ijpeds.v14.i1.pp153-166.

[31] S. Aissou, E. Amirouche, K. Iffouzar, K. Ghedamsi, and D. Aouzellag, "Online position error correction technique for sensorless control of multipole permanent magnet machines," *International Journal of Power Electronics and Drive Systems*, vol. 14, no. 4, pp. 1929–1936, Dec. 2023, doi: 10.11591/ijpeds.v14.i4.pp1929-1936.

[32] N. A. Windarko *et al.*, "Hybrid photovoltaic maximum power point tracking of Seagull optimizer and modified perturb and observe for complex partial shading," *International Journal of Electrical and Computer Engineering*, vol. 12, no. 5, pp. 4571–4585, Oct. 2022, doi: 10.11591/ijece.v12i5.pp4571-4585.

BIOGRAPHIES OF AUTHORS

Dattatray Surykant Sawant ⓘ � SC ⓒ received the B.E. degree from Mumbai University, India, in 2008, the M. E. degree from Sardar Patel Institute of Technology, Mumbai, India, in 2013, and is currently working toward the Ph.D. degree with the Sardar Patel Institute of Technology, Mumbai, India, in the Department of Electronics and Telecommunication Engineering. Since 2014, he has been with the SVKM's NMIMS Mukesh Patel School of Technology Management and Engineering, Mumbai, India as Assistant Professor. His research interests include digital controller for power electronic systems, control systems, communication systems, robotics and automation. He can be contacted at email: dssawant1@gmail.com.

Yerramreddy Srinivasa Rao ⓘ 🔾 SC ⓒ received the Ph.D. degree in power electronics from the Indian Institute of Technology Bombay, Mumbai, India, in 2010. He has a work experience of more than ten years in the industry. He has been in the teaching profession for more than 28 years, of which he has been associated with the Bhartiya Vidya Bhavan's Sardar Patel College of Engineering and subsequently, Sardar Patel Institute of Technology for more than 20 years. He was the Head of the Department several times and is currently the Vice-Principal as well as the Dean of R&D Department at Sardar Patel Institute of Technology, Mumbai, India. His major research publications are in embedded systems, digital power electronics, and communication systems. He can be contacted at email: ysrao@spit.ac.in.

Rajendra Ramchandra Sawant ⓘ 🔾 SC ⓒ received the B.Eng. degree from the Government College of Engineering, Marathwada University, Aurangabad, India, in Jul. 1988, and the M.Tech. and Ph.D. degrees from the Indian Institute of Technology Bombay, Mumbai, India, in Jul. 1996 and Feb. 2009, respectively, all in electrical engineering. He has been engaged as Power Electronics Consultant to various small- and medium-scale companies in Mumbai and Pune region since 1998 and has been involved in the design and development of different industrial products in Induction Heating Systems and Power Conditioning. He was engaged in university-level academic teaching on different teaching positions in the field of electrical engineering for the last 28 years, with different universities in India. He is currently with the Department of Electronics and Telecommunications, Sardar Patel Institute of Technology, Mumbai, India, as a professor. His research interests include smart controllers for induction heating system, renewable energy, power-quality improvements, and fast-battery charging technologies for modern electric vehicles. He can be contacted at email: rajendra.sawant@spit.ac.in.